Available online at www.sciencedirect.com

ScienceDirect

Journal of the European Ceramic Society 29 (2009) 697–702

www.elsevier.com/locate/jeurceramsoc

The synthesis and sintering behaviour of $BaZr_{0.9}Y_{0.1}O_{3-\delta}$ powders prepared by spray pyrolysis

Paul A. Stuart[a], Toshiyuki Unno[c], Renata Ayres-Rocha[b], Elisabeth Djurado[b], Stephen J. Skinner[a,*]

[a] *Department of Materials, Imperial College London, Exhibition Road, London SW7 2AZ, United Kingdom*
[b] *LEPMI – ENSEEG, 1130 Rue de la Piscine, BP 75, 38402 St. Martin d'Hères cedex, France*
[c] *Department of Metallurgy and Ceramics Science, Tokyo Institute of Technology, S8-11, 2-12-1, O-okayama, Meguro-ku, Tokyo 152-8552, Japan*

Received 3 June 2008; accepted 9 July 2008
Available online 23 August 2008

Abstract

Powders of $BaZr_{0.9}Y_{0.1}O_{3-\delta}$ (BZY10) were synthesised by spray pyrolysis from nitrate salt solutions for the first time. Differences in the powders produced were explored when the concentration of solution, atomisation frequency, aerosol flow rate and furnace temperature were varied. X-ray powder diffraction (XRD) was used to determine that powders produced using a furnace temperature of 800 °C were of single phase. Powder that was produced using a higher atomisation frequency and a lower salt solution concentration resulted in a favourable particle size distribution and morphology for sintering. A density of approximately 91% of the theoretical density (TD) was achieved by sintering at 1500 °C for 1 h in flowing air, significantly higher than is achieved with commercial BZY10 powders using these conditions. This constitutes a significant lowering of the sintering temperature of this oxide.

Keywords: $BaZrO_3$-Y; Sintering; Proton conductor; Spray pyrolysis

1. Introduction

Acceptor-doped perovskites have been shown to exhibit proton conduction in humid atmospheres at high temperature.[1] These materials are used to conduct hydrogen ions across gas impermeable membranes in devices such as solid oxide fuel cells and gas sensors. Consequently, these materials are often required to be prepared to a high density to prevent gas diffusion across the membrane. Some of the most intensively investigated proton conductors are based on barium zirconate, $BaZrO_3$, and barium cerate, $BaCeO_3$. It is acknowledged that the doped barium cerates exhibit a higher total conductivity than the doped barium zirconates,[2] however, additional figures of merit must be considered when selecting an electrolyte material for solid oxide proton conducting fuel cells (SOFCs). Indeed it has been shown by Kreuer[3] that the barium zirconates exhibit higher bulk conductivity than the cerates, despite having lower total conductivity, combined with greater chemical and mechanical stability than the cerates.[4] In particular, the stability of the cerates with respect to carbonate formation in typical fuel cell operating atmospheres is of concern.[5]

BZY10 is notoriously difficult to produce with high density and is quoted as requiring extreme conditions such as sintering at 1700 °C for 24 h[2,6,7] to achieve a density of >95%TD. Snijkers et al.[8] synthesised BZY10 by solid-state reaction. In this work, pellets of BZY10 were iso-statically pressed at 400 MPa and subsequently sintered in air for 4 h at temperatures between 1500 °C and 1700 °C. They report a final sintered density of 94.96%TD ($TD = 6.16\ g\ cm^{-3}$), although it was not clearly stated in the paper which sintering temperature this value corresponded to. We assume that this was the maximum density achieved and therefore, that this value corresponded to a 1700 °C sintering temperature. Such high sintering temperatures are undesirable, as these materials are required to be co-sintered with electrode materials to form cells. The sintering temperatures of typical electrode materials are much lower than 1700 °C and as

---

[*] Corresponding author. Tel.: +44 20 7594 6782; fax: +44 20 7594 6757.
E-mail address: s.skinner@imperial.ac.uk (S.J. Skinner).

0955-2219/$ – see front matter © 2008 Elsevier Ltd. All rights reserved.
doi:10.1016/j.jeurceramsoc.2008.07.004

electrodes are also required to have a certain amount of porosity, a sintering temperature much lower than 1700 °C is needed. A further development was reported by Babilo et al.[9] on the BZY20 sample, where a reduction to 1600 °C was reported with a sintering time of 10 h required to achieve density higher than 95% of theoretical. The aim of the current work is to produce a pure BZY10 powder that will sinter to a high density at the lowest temperature possible.

Nanocrystalline oxide powders have previously been synthesised by spray pyrolysis.[10–14] These powders typically have a submicron average particle size and are formed of dense spheres. We hypothesise that BZY10 powders produced by spray pyrolysis will have a particle size distribution and morphology that may have a beneficial effect on the sintering behaviour of the material.

2. Experimental

An aqueous solution of $Ba(NO_3)_2$ (R.P. Normapur, 99.5% purity), $ZrO(NO_3)\cdot 6H_2O$ (Fluka, >97%) and $Y(NO_3)_3\cdot 4H_2O$ (Aldrich, 99.999%) was prepared in cationic proportion 10:9:1, respectively. An ultrasonic atomiser was used to create an aerosol from this solution and synthetic air was used to carry the aerosol through a 2-zone tubular furnace. The first zone of the furnace that the aerosol experienced was 50 °C lower than the second. The oxide powder particles formed were collected electrostatically in an extension of the tube outside of the furnace. Full details of the experimental setup are described in Ref. [10]. The effects of varying solution concentration, nebulisation frequency, carrier gas flow rate and furnace temperature were explored. Further experimental details are listed in Table 1.

Powders produced were characterised using XRD (PANalytical X'pert Pro MPD) and analysed using high-resolution field emission scanning electron microscopy (FE-SEM, ZEISS ultra 55). A JEOL FX2000 transmission electron microscope (TEM) with a tungsten filament was operated in bright field mode at an accelerating voltage of 200 kV to obtain TEM micrographs of powder samples. Sintering behaviour was determined using a Netzsch DIL 402 dilatometer with a heating rate of 10 °C min^{-1} in a flowing air atmosphere. Additionally, the particle size distributions (PSD) of the milled commercial powder and of a sample produced by spray pyrolysis were determined using a Malvern Mastersizer 2000 laser diffractometer.

Pellets, 6 mm in diameter, were created by uniaxial pressing of the powders at ∼170 MPa. These were heated to 1500 °C, held at this temperature for 1 h and subsequently allowed to cool at a natural rate. In addition to the powders prepared by spray pyrolysis, pellets of 6 mm in diameter were prepared from BZY10 commercial powder supplied by Praxair that had been milled for 120 h, with and without a 1-wt% ZnO additive. A ZnO additive has previously been shown to act as a sintering aid with BZY powders and was therefore included in this study.

Table 1
Experimental details for sample preparation

No.	Solution concentration ($mol\,l^{-1}$)	Flow rate ($l\,min^{-1}$)	Nebulisation frequency (MHz)	Temperature (°C)
1	2.5×10^{-2}	6	2.5	600
2	2.5×10^{-2}	6	1.7	600
3	2.5×10^{-2}	6	1.7	800
4	2.5×10^{-2}	6	2.5	800
5	2.5×10^{-3}	6	1.7	800
6	2.5×10^{-3}	6	2.5	800

3. Results and discussion

3.1. Synthesis and characterisation

The XRD pattern of the initial powder produced (Fig. 1(a)), revealed the existence of a barium zirconate perovskite phase with a secondary $Ba(NO_3)_2$ phase present. In our initial experiments the furnace temperature was 600 °C (Table 1) which is very close to the decomposition temperature of 599 °C for the $Ba(NO_3)_2$ precursor as found by differential thermal analysis (DTA) (see Fig. 1(a) inset). When the furnace temperature was raised to 800 °C, the $Ba(NO_3)_2$ precursor fully decomposed

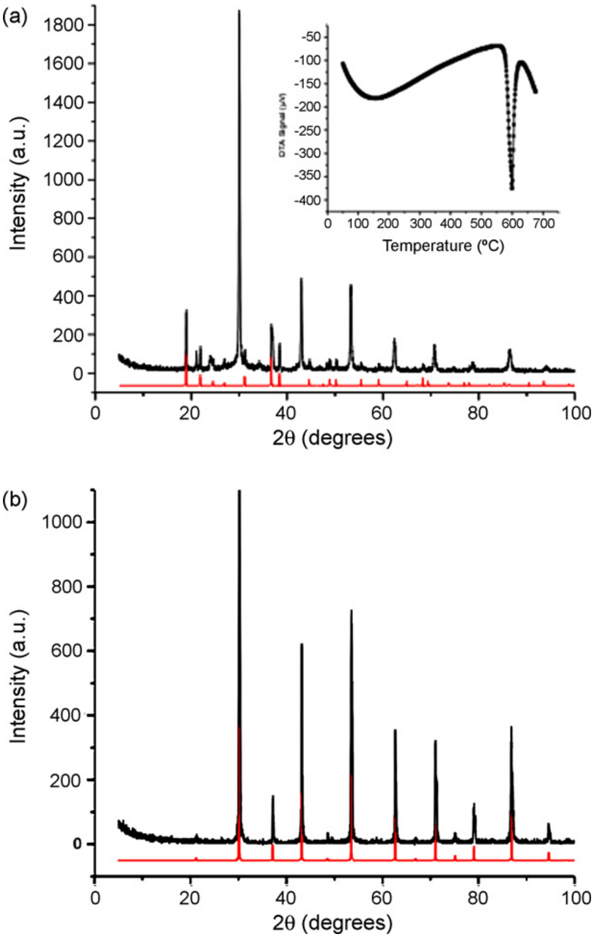

Fig. 1. (a) XRD powder diffraction pattern of a sample produced by spray pyrolysis at 600 °C—markers below diffraction pattern indicate $Ba(NO_3)_2$ peak positions.[17] Inset, graph showing DTA signal against temperature for $Ba(NO_3)$ precursor. (b) XRD powder diffraction pattern of a sample produced by spray pyrolysis at a furnace temperature of 800 °C showing single phase BZY10. Markers below diffraction pattern indicate $BaZrO_3$ peak positions.[18]

leaving a single barium zirconate perovskite phase (Fig. 1(b)) indicating that the production of BZY by spray pyrolysis is limited by the decomposition temperature of the precursors used. Hence through judicious choice of precursor the BZY phase can be prepared at remarkably low temperatures.

The total residence time of the aerosol within the tube furnace could be altered by changing the carrier gas flow rate and hence the decomposition of the precursor could be controlled at temperatures just above the decomposition temperature by ensuring that the material remained in the pyrolysis chamber for longer time periods. In further syntheses the furnace temperature was maintained at 600 °C but the carrier gas flow rate was lowered from 6 l/min to 3 l/min, increasing the precursor residence time. The resultant powders still contained $Ba(NO_3)_2$ but a reduction in the relative intensity of XRD peaks attributable to $Ba(NO_3)_2$ was observed, suggesting that the longer residence time allowed further decomposition of the nitrates to occur. Whilst this is of note it should be considered that the spray pyrolysis process produces powder at a relatively slow rate, and as the powder yield rate is directly proportional to the carrier gas flow rate, it was deemed undesirable to decrease the carrier gas flow rate below 3 l/min to produce single phase materials. Therefore, to ensure maximum powder production with full conversion of starting materials, a furnace temperature greater than 600 °C was selected to form a single perovskite phase material. The production of BZY10 powders at 800 °C is, therefore, a significant decrease in the synthesis temperature and considerably lower than recently reported by D'Epifanio et al.[13] It is also interesting to note that the introduction of Y to the precursors does not result in problems of inhomogeniety. Bucko and Oblakowski[14] found that the crystallite size of $BaZrO_3$ prepared by spray pyrolysis decreased with an increase in furnace temperature. They comment that the kinetics of the formation of the $BaZrO_3$ phase from the precursor salts are the probable cause for this furnace temperature effect. It was argued that the degree of overheating increased with a higher furnace temperature, causing the crystal nucleation process to be more energetically favourable than crystal growth. It may therefore be desirable to increase the synthesis to temperatures above 800 °C depending on the application.

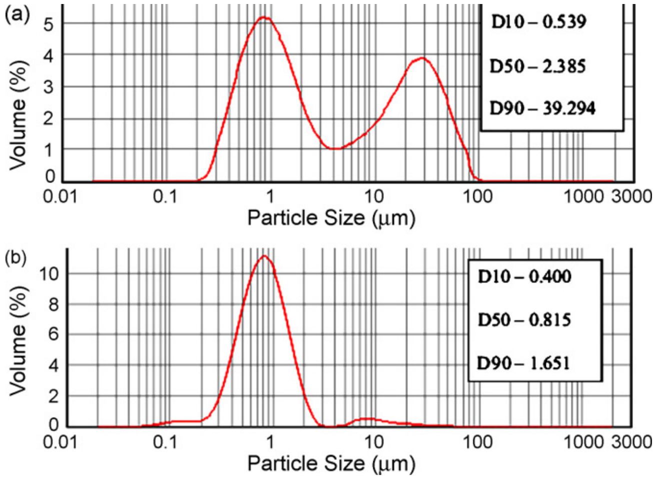

Fig. 2. (a) Particle size distribution of milled commercial powder and (b) particle size distribution of powder prepared by pyrosol synthesis, 2.5×10^{-3} mol l^{-1}, 2.5 MHz, 800 °C.

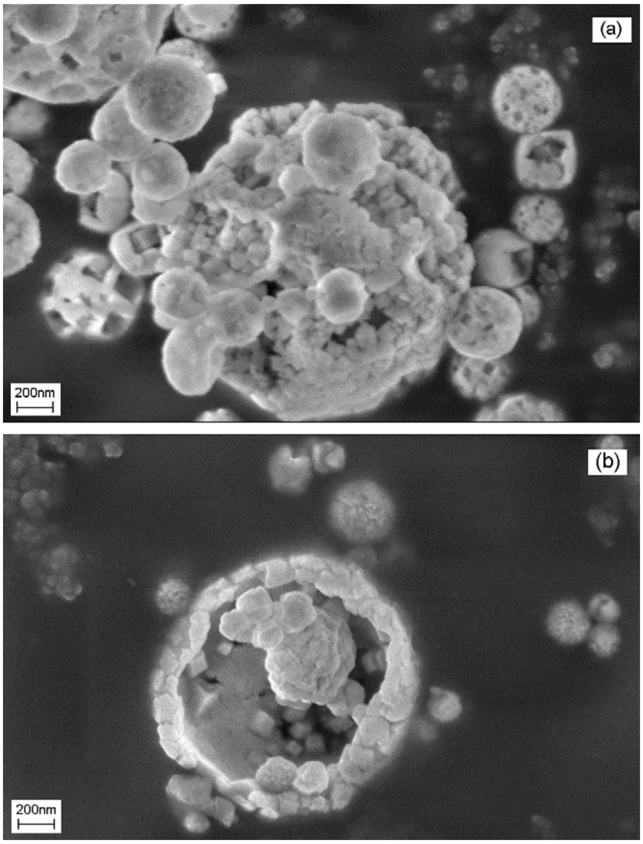

Fig. 3. (a) SEM micrograph of powder showing typical particle agglomeration and faceted particles that are present in all samples. (b) SEM micrograph of powder prepared by pyrosol synthesis, 2.5×10^{-3} mol l^{-1}, 2.5 MHz, 800 °C showing particle size distribution and varied particle morphologies.

The sintering process of ceramic powders is widely recognised to be aided by the presence of small and dense particles. Fig. 2(a) and (b) displays particle size distributions (PSDs) with corresponding d10, d50 and d90 values for the milled commercial BZY10 powder and BZY10 powder produced by spray pyrolysis at a furnace temperature of 800 °C, respectively. Both PSDs show a peak at around 0.8–0.9 µm although this peak is narrower for the pyrolysis sample, indicating a lower distribution of particle sizes. A second mode is observed for the PSD of the commercial powder at around 30 µm that is not observed for the pyrolysis sample and this is reflected in the large difference in d90 values between the two samples. A shoulder present on the main peak in the PSD for the material produced by spray pyrolysis indicates a low volume percent of very small particles, the presence of which was confirmed by electron microscopy. SEM and TEM imaging of spray pyrolysis samples suggests that particles above and around the d50 value in size are in fact agglomerations of smaller particles (Fig. 3(a) and (b) and Fig. 4(a)). A secondary peak at around 10 µm in the PSD of the spray pyrolysis sample suggests the presence of larger agglomerates although this could not be verified using SEM imaging. It may be that the particle size analyser was unable to measure the size of particles and agglomerates accurately due to

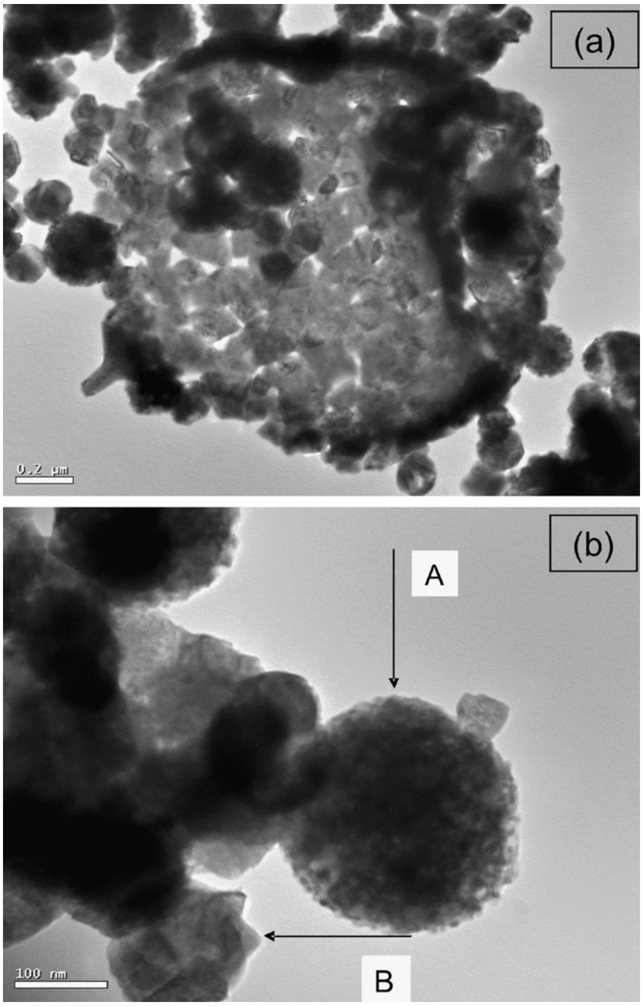

Fig. 4. (a) TEM micrograph of powder showing an agglomeration of particles less than 250 nm in diameter. Scale bar represents 0.2 µm and (b) TEM micrograph of powder exhibiting the presence of dense particles. Scale bar represents 100 nm.

the presence of insufficiently separated clusters of powder. In an attempt to break up agglomerates, an ultrasonic probe was operated when submerged in a suspension that contained powder produced by spray pyrolysis. SEM imaging confirmed that agglomerates were broken up by this procedure, although the increase in the final sintered density using a sample synthesised from this powder was minimal.

Fig. 3(a) and (b) are SEM micrographs of a powder sample produced at 800 °C, 2.5 MHz with a solution concentration of 2.5×10^{-3} mol l^{-1}, and shows the irregular particle morphologies produced. Morphologies of these types were observed in all materials produced by spray pyrolysis. Many particles appear to have square facets on their surface with some having adopted a cuboidal shape. It is not known whether the cubic crystal structure of BZY10 was responsible for these morphological features. Possibly, preferential crystal growth occurred after particle nucleation and this caused the formation of cuboidal crystallites. Fig. 3(a) and (b) also features agglomerations of particles that are common within all spray pyrolysis powder samples studied. The agglomerate in Fig. 3(b) appears to be filled with particles, whereas Fig. 3(a) suggests that some agglomerates are hollow. Transmission electron microscopy was therefore used to determine the density of particles and the density of these commonly found agglomerates. A TEM micrograph of the same powder is shown in Fig. 4(a) and is evidence that agglomerates, typically 1 µm in diameter, are generally a collection of particles of less than 250 nm diameter that form one single hollow sphere. Mass thickness contrast is thought to cause the majority of agglomerates to appear as dark rings encompassing regions of brighter contrast. This indicates that mass is unevenly distributed throughout the cross-section of the agglomerate and that these agglomerates are therefore hollow. Fig. 4(b) displays two further types of particle morphology, commonly observed, that are not agglomerates of the type previously mentioned. Particle A in Fig. 4(b) appears to be a dense particle formed from many, very small crystals, less than 10 nm across and may perhaps be classed as an agglomerate. Particle B in Fig. 4(b) appears as a dense particle formed from several angular crystals, of approximately 70 nm dimension.

3.2. Sintering behaviour

Dilatometric curves of samples produced under a range of conditions are presented in Fig. 5. It is important to note the green density of the samples (Table 2) when comparing dilatometric curves as the dilatometer measures change in sample length. The onset of sintering occurs at around 1200 °C for each spray pyrolysis produced sample, however, small differences in the onset temperature may have been discernable if a slower heating rate (<10 °C min^{-1}) had been used. From a comparison of the dilatometric curves for the samples produced at 1.7 MHz and 2.5 MHz nebulisation frequency, it was observed that increasing the atomising frequency alone did not significantly increase the final sintered density. Further details of the influence of spray pyrolysis parameters on the particle morphology and sintering behaviour of yttria stabilised zirconia were

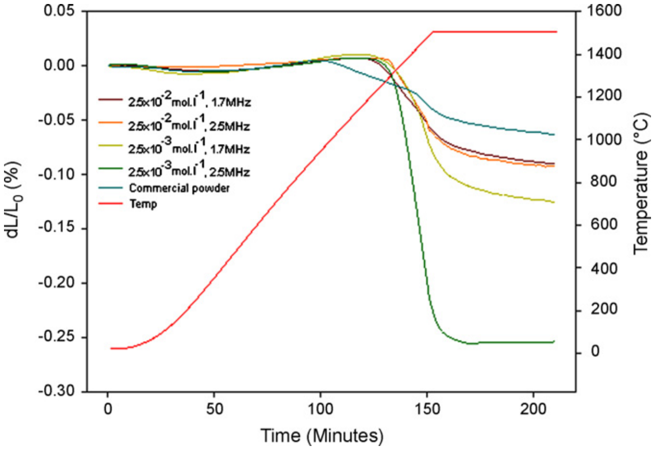

Fig. 5. Dilatometric curves measured between room temperature and 1500 °C for samples produced under varying spray pyrolysis conditions and a sample produced using commercial powder. Arrows indicate which axis data is relevant to. Legend includes solution concentration and nebulisation frequency values for each experiment. The furnace temperature and flow rate conditions were same for all spray pyrolysis samples.

Table 2
Green and sintered densities of pellets produced using powders from spray pyrolysis experiments and doped and non-doped commercial powder

Sample	Green density of dilatometry sample (%TD)	Sintered density (%TD)
1	32.5	41.5
2	40.8	43.0
3	35.3	42.4
4	35.7	45.4
5	37.3	54.0
6	37.6	90.6
Commercial powder	50.1	59.0
ZnO doped	50.7	91.5

reported by Gaudon et al.[15] In this study, it was reported that the PSD widened and the average particle size decreased when the atomising frequency was increased. Furthermore, they state that the atomising frequency is the most influential parameter for control of the droplet size of the aerosol and that ceramic materials will sinter more easily with a wider distribution of particle sizes. We conclude that it is unlikely that the particle size distributions of our powders were significantly effected by an increase in atomising frequency from 1.7 MHz to 2.5 MHz as the increase in the final sintered density observed was minimal.

As frequency was not found to have a significant effect on the final sintered density, the effect of concentration was investigated. Hence two concentrations and two frequencies were investigated (2.5×10^{-3} mol l^{-1} and 2.5×10^{-2} mol l^{-1} at 1.7 MHz and 2.5 MHz). The powder produced at low concentration and low frequency achieved a final density of approximately 54%TD, whereas the powder synthesized from higher concentration solution at 1.7 MHz only reached a final sintered density of approximately 41.5%TD. Bucko and Oblakowski[14] prepared non-doped $BaZrO_3$ nanopowders by spray pyrolysis and found that the PSD was significantly affected by the solution concentration. In their work, the average particle size varied from 90 nm to 500 nm in powders prepared from solutions of 0.001 M at 1200 °C and 0.1 M at 800 °C, respectively. We therefore conclude that a change in solution concentration had a greater affect on the sintering behaviour, and PSD, of our powders produced by spray pyrolysis than changes in atomising frequency. An atomising frequency of 2.5 MHz and a solution concentration of 2.5×10^{-3} mol l^{-1} were selected as the combination most likely to result in an increase in sintered density and these samples were found to sinter to a final density of 90.6%TD. The combination of a high atomising frequency and a low solution concentration resulted in dramatically improved final sintered density.

Particle morphology, as well as PSD characteristics, may play a major role in the sintering behaviour of BZY10. From observations made using SEM and TEM, any one spray pyrolysis powder sample appears to include a variety of particle and agglomeration morphologies. This variation was perhaps linked to the range of droplet size and shape produced by the ultrasonic atomiser. For example, particle A in Fig. 4(b) may have been formed by many small droplets agglomerating together before nucleation with little growth subsequently occurring, whereas larger droplets may have experienced a different nucleation and growth mechanism to form particle B in Fig. 4(b). The proportions of these differing morphologies within any one sample were difficult to quantify and hence the influence of a higher proportion of a particular morphology over another on the sintering behaviour is unknown. Djurado and Meunier[10] studied the effect that atomising frequency had on the synthesis of zirconia powders produced by spray pyrolysis. They observed a roughening of particle surfaces when the nebulising frequency was decreased from 1.7 MHz to 850 kHz. This change in particle morphology was attributed to an increase in the rate of solvent evaporation from the aerosol. A variation of parameters in the current study may have also affected the manner in which the aerosol was transformed into oxide powder and hence alter the particle morphology.

The final density for each sample would perhaps be further increased by isostatically pressing the pellet samples at 300 MPa before the sintering process is carried out. An increase in sintering time would be unlikely to improve the final density of the material as a constant dL/L_o was observed during the 1-h isotherm. This therefore represents a significant reduction in both sintering temperature and time in comparison with the current literature data.[6,8] Evidently the microstructure of the material may be altered by increasing the sintering time and this could affect the electrochemical properties of the sample.

Samples created using milled commercial BZY10 powder reached a final density of about 59%TD and clearly had different sintering behaviour to the spray pyrolysis samples. The onset of sintering occurred at a lower temperature, approximately 1000 °C, and the sample appeared to have additional phases of sintering. This is indicative of the very different PSD and particle morphology of the powder compared to the spray pyrolysis produced powders. The samples containing a 1-wt% ZnO additive reached a final density of about 91.5%TD. Clearly, a dramatic increase in the final density occurred when 1 wt% ZnO was added to the commercial powder. This finding is in accordance with Babilo and Haile[6] and Tao and Irvine.[16] It is of interest to note that the final sintered density of the powder produced by spray pyrolysis and that produced with a ZnO additive are in close agreement indicating that the synthesis method outlined in this work will produce powders of suitable initial morphology for use in ceramic proton conducting devices.

4. Conclusions

It was found that a furnace temperature greater than 600 °C was required to synthesise single phase BZY10 successfully using spray pyrolysis. Variation of spray pyrolysis parameters affected the powders produced and hence altered their sintering behaviour. A high ultrasonic atomising frequency and a low solution concentration were discovered to be required to produce a pure BZY10 powder that sintered to form a highly dense pellet at 1500 °C. By synthesising a BZY10 powder using spray pyrolysis a significant improvement in final sintered density was achieved over a milled commercial BZY10 powder. We found that the commercial powder had a higher average particle size than the spray pyrolysis powder and that this contributed to the improved sintered density observed. The influence of various particle morphologies on the sintering behaviour of spray pyrolysis samples was not discernable due to the difficulty in quantifying proportions of any one particular particle morphology.

Acknowledgements

The authors would like to thank Denis Cummings for his assistance with particle size measurements, Alexander Jasper for assistance with TEM imaging and the British Council, Paris and UKERC for funding. R. A. Rocha acknowledges CNPq - Brazil for funding for her post-doctoral position at LEPMI (France).

References

1. Azad, A. K. and Irvine, J. T. S., Synthesis, chemical stability and proton conductivity of the perovksites $Ba(Ce,Zr)_1 - x\,Scx\,O_3 - \delta$. *Solid State Ionics*, 2007, **178**(7–10), 635–640.
2. Ryu, K. H. and Haile, S. M., Chemical stability and proton conductivity of doped $BaCeO_3$–$BaZrO_3$ solid solutions. *Solid State Ionics*, 1999, **125**, 355–367.
3. Kreuer, K. D., Proton Conducting Oxides. *Annu. Rev. Mater. Res.*, 2003, **33**, 333–359.
4. Iwahara, H., Technological challenges in the application of proton conducting ceramics. *Solid State Ionics*, 1995, **77**, 289–298.
5. Zakowsky, N., Williamson, S. and Irvine, J. T. S., Elaboration of CO_2 tolerance limits of BaCe0.9Y0.1O3–δ electrolytes for fuel cells and other applications. *Solid State Ionics*, 2005, **176**, 3019–3026.
6. Babilo, P. and Haile, S. M., Enhanced Sintering of Yttrium-Doped Barium Zirconate by Addition of ZnO. *J. Am. Ceram. Soc.*, 2005, **88**, 2362–2368.
7. Schober, T. T. and Bohn, H. G., Water vapor solubility and electrochemical characterization of the high temperature proton conductor BaZr0.9Y0.1O2.95. *Solid State Ionics*, 2000, **127**, 351–360.
8. Snijkers, F. M. M., Buekenhoudt, A., Cooymans, J. and Luyten, J. J., Proton conductivity and phase composition in BaZr0.9Y0.1O3−δ. *Scripta Mater.*, 2004, **50**, 655–659.
9. Babilo, P., Uda, T. and Haile, S. M., Processing of yttrium-doped barium zirconate for high proton conductivity. *J. Mater. Res.*, 2007, **22**, 1322–1329.
10. Djurado, E. and Meunier, E., Synthesis of Doped and Undoped Nanopowders of Tetragonal Polycrystalline Zirconia (TPZ) by Spray-Pyrolysis. *J. Solid State Chem.*, 1998, **141**, 191–198.
11. Poirson, A., Decorse, P., Caboche, G. and Dufour, L. C., A dilatometric study of the $La0.8Sr0.2MnO_3$ sintering behaviour. *Solid State Ionics*, 1997, **99**, 287–295.
12. Menzler, N. H., Lavergnat, D., Tietz, F., Sominski, E., Djurado, E., Fischer, W. *et al.*, Materials synthesis and characterization of 8YSZ nanomaterials for the fabrication of electrolyte membranes in solid oxide fuel cells. *Ceram. Int.*, 2003, **29**, 619–628.
13. D'Epifanio, A., Fabbri, E., Di Bartolomeo, E., Licoccia, S. and Traversa, E., Design of BaZr0.8Y0.2O3-d Protonic Conductor to Improve the Electrochemical Performance in Intermediate Temperature Solid Oxide Fuel Cells (IT-SOFCs). *Fuel Cells*, 2008, **1**, 69–76.
14. Bucko, M. M. and Oblakowski, J., Preparation of $BaZrO_3$ nanopowders by spray pyrolysis method. *J. Eur. Ceram. Soc.*, 2007, **27**, 3625–3628.
15. Gaudon, M., Djurado, E. and Menzler, N. H., Morphology and sintering behaviour of yttria stabilised zirconia (8-YSZ) powders synthesised by spray pyrolysis. *Ceram. Int.*, 2004, **30**, 2295–2303.
16. Tao, S. and Irvine, J. T. S., Conductivity studies of dense yttrium-doped $BaZrO_3$ sintered at 1325 °C. *J. Solid State Chem.*, 2007, **180**, 3493–3503.
17. Nowotny, H. and Heger, G., Structure refinement of strontium nitrate, $Sr(NO_3)_2$, and barium nitrate, $Ba(NO_3)_2$. *Acta Crystallograph. C*, 1983, **39**, 952–956.
18. Levin, I., Amos, T. G., Bell, S. M., Farber, L., Vanderah, T. A., Roth, R. S. *et al.*, Phase equilibria, crystal structures, and dielectric anomaly in the $BaZrO_3$–$CaZrO_3$ system. *J. Solid State Chem.*, 2003, **175**, 170–181.